

INSTABILITY OF GRAVITY TYPE QUAY WALL INDUCED BY LIQUEFACTION OF BACKFILL DURING EARTHQUAKE

EIJI KOHAMAⁱ⁾, KINYA MIURAⁱⁱ⁾, NOZOMU YOSHIDAⁱⁱⁱ⁾,
NATSUHIKO OHTSUKA^{iv)} and SATORU KURITA^{v)}

ABSTRACT

The mechanism of the damage to a gravity type quay wall caused by liquefaction of the backfill ground during an earthquake is made clear through a shaking table test and theoretical examination. A series of model shaking table tests was conducted focusing on the occurrence of liquefaction in the backfill ground. The movement of the caisson is found to be quite different depending on whether liquefaction occurred in the backfill ground or not. The fluctuating earth pressure on the caisson suppresses the movement of the caisson when liquefaction does not occur. On the other hand, sliding of the caisson is enhanced since the fluctuating component of earth pressure and the inertial force coincide in phase angle when liquefaction occurs in the backfill ground. When liquefaction occurs, observed earth pressure agrees with that evaluated by Westergaard's formula originally derived for the water pressure on the dam.

The fluctuating earth pressure acting on the back wall of the caisson in the process to liquefaction was carefully observed in the model shaking tests. It was found that the amplitude of the earth pressure first decreased to a very small value because of the reduction of the stiffness of the backfill due to the excess pore water pressure generation, and then increased because the phase angle of the earth pressure changed 180 degrees. This indicates that stability criteria of the caisson should be developed not by the onset of the liquefaction but by the sudden phase change. This feature is demonstrated by the simplified mass-spring-dashpot model proposed by the authors.

Key words: earth pressure, earthquake, gravity type quay wall, liquefaction, shaking table model test, sliding (IGC: E8)

INTRODUCTION

Significant damage has occurred in port and harbor facilities, especially those in reclaimed lands, during recent large earthquakes in Japan. The function of quay walls was frequently lost because gravity type quay wall caissons were displaced toward the sea and subsided. It seems that the damage was enhanced by the occurrence of liquefaction in the backfill (e.g., JGS, 1994; Inagaki et al., 1996; Kamon et al., 1996). Actually, close examination of the damage to quay walls in Hokkaido Island, Japan, during three recent big earthquakes, i.e., 1993 Kushiro-oki, 1993 Hokkaido Nansei-oki and 1994 Hokkaido Toho-oki earthquakes, clarified that the degree of damage is strongly related to the occurrence of liquefaction in the backfill ground (JGS, 1994; Hokkaido Development Bureau, 1996). A clear proof of the effect of liquefaction on the stability of quay walls is seen in the

damage to treated quay walls. Remedial measures against liquefaction were positively made in Hokkaido Island after the 1983 Nihonkai-chubu earthquake; the backfill ground of quay walls was improved by a combination of sand compaction pile and gravel drain methods. They survived large earthquakes with little or no damage, in marked contrast to the severe damage frequently seen to quay walls with non-treated backfill ground.

Quay walls are damaged because of the following factors:

- Inertial force acting on the caisson
- Earth pressure acting on the back of the quay wall
- Reduction of the bearing capacity of the foundation ground

Inertial force is a body force induced by vibration through the foundation, whose magnitude fluctuates depending on the acceleration input. Both static and fluctuating components of the earth pressure act on the back

ⁱ⁾ Graduate Student, GeoMechanics Group, Division of Structural and Geotechnical Engineering, Graduate School of Engineering, Hokkaido University, Sapporo, Hokkaido 060-0813.

ⁱⁱ⁾ Associate Professor, ditto.

ⁱⁱⁱ⁾ General Manager, Engineering Research Institute, Sato Kogyo Co. Ltd., Tokyo.

^{iv)} General Manager, Engineering Department, North Japan Port Consultants Co. Ltd., Sapporo, Hokkaido.

^{v)} Senior Officer, Department of Ports and Harbors, Hokkaido Development Bureau, Sapporo, Hokkaido.

Manuscript was received for review on June 27, 1997.

Written discussion on this paper should be submitted before July 1, 1999 to the Japanese Geotechnical Society, Sugayama Bldg. 4F, Kanda Awaji-cho, 2-23, Chiyoda-ku, Tokyo 101-0063, Japan. Upon request the closing date may be extended one month.

wall of the caisson. The fluctuation of the earth pressure is a result of the interactive behavior between the vibrations of the caisson and the backfill ground. Therefore a combination of the inertial force and earth pressure may result in the complicated behavior of the caisson, which is the main interest in this paper.

The effect of the reduction of the bearing capacity of the foundation ground may also be important as seen, for example, in the damage during the 1995 Hyogoken-nambu earthquake, where many quay walls were severely damaged by the loss of the bearing capacity of the foundation sand as well as by liquefaction of the backfill (Inagaki et al., 1996; and Kamon et al., 1996). However, this is not investigated in this paper in order to make the discussion simple.

Earth pressure acting on a retaining wall during an earthquake is usually evaluated by the seismic coefficient method proposed by Okabe (1924) and Mononobe (1929) in engineering practice, where the static inertial force is employed instead of the fluctuating acceleration. As pointed out by Ichihara and Matsuzawa (1972), the transient earth pressure is not taken into account and consistent plastic equilibrium condition is not guaranteed in the backfill in this pseudo static method. Matsuo (1941) measured the distribution of the earth pressure during an earthquake in model tests, and emphasized the significance of the relationship of the natural frequencies of structures and ground with the dominant frequency of the earthquake. Iwatate et al. (1982, 1984) conducted a series of model shaking table tests on buried rigid structures, and derived the following:

- Earth pressure during shaking is much dependent on the fixity condition of the structure.
- Fluctuating earth pressure is rather small compared with that predicted by the seismic coefficient method over a wide range of acceleration intensity if the ground does not go into plastic state.
- When the ground liquefies, the earth pressure fluctuates more; this is similar to fluid pressure acting on a vibrating object.

Kazama and Inatomi (1990) demonstrated the fluctuation of earth pressure on a rigid structure in a series of model shaking table tests using a dry sand deposit. They proposed a rigid body-spring-dashpot model to simulate the behavior of a structure subjected to dynamic earth pressure.

Past research has indicated the importance of considering the interactive behavior between the quay wall caisson and backfill ground in a dynamic manner. It is also known that the behavior is quite different depending on whether the backfill liquefies or not. The interactive behavior, however, cannot be said to be clear or well recognized. For example, partly liquefied ground or transient behavior to liquefaction in the backfill have not been treated in past research.

This study aims to clarify the mechanism of the damage to gravity type quay walls during an earthquake by focusing on the occurrence of liquefaction in the backfill ground. The behavior of the quay wall during the

vibration is investigated through a series of model shaking table tests and through analysis considering the interactive behavior between the inertial force and earth pressure from the backfill. The transient behavior of the earth pressure in the process to liquefaction is also investigated experimentally and analytically.

TEST METHOD

Model, Container and Shaking Table

A typical section of an actual gravity type quay wall is shown in Fig. 1; the caisson rests on the rubble mound and the small section of the backfill is assigned to the gravelly soils. The rubble mound is effective for the dispersion of the dead weight of the caisson and improves the bearing capacity of the foundation ground. The gravelly material in the backfill is used to prevent the backfill material from being washed away and to reduce the active earth pressure by its large internal friction angle. Since the interactive behavior between the caisson and the backfill ground is mainly investigated in this study, existence of the rubble mound was ignored in the tests. In addition, the gravelly material in the backfill is not considered in the interests of simplicity in grasping the behavior.

The gravity type quay wall used in the shaking table tests is shown in Fig. 2(a). The caisson was placed directly on the level base ground inside a rigid container composed of steel members and glass plates. The caisson was a hollow box made of steel plates, in which lead balls were stuffed so that the total mass of the caisson was 50 kg, resulting in average density of 2.2 t/m³. Foam rubber plates 8 mm thick, and coated with silicon grease, were placed at the ends of the caisson in order to prevent the wash away of the backfill material and to reduce the friction between the caisson and the side walls of the container. It has a density of 0.19 g/cm³, nominal Young's modulus of about 40 kPa, and negligibly small Poisson's ratio. Foam rubber plates 5 cm thick were also attached to the side walls of the container on the transversal side. The effect of the foam rubber plate on the reduction of the reflection of the waves propagating in the base and backfill was confirmed in the preliminary test. A thick percolate mat made of entangled plastic wires was set as a breakwater in order to reduce the reflection of the wave through water on the opposite side of the caisson. A con-

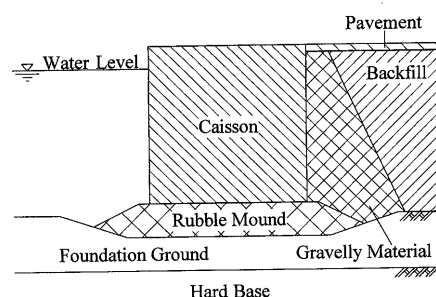


Fig. 1. Typical cross section of gravity type quay wall

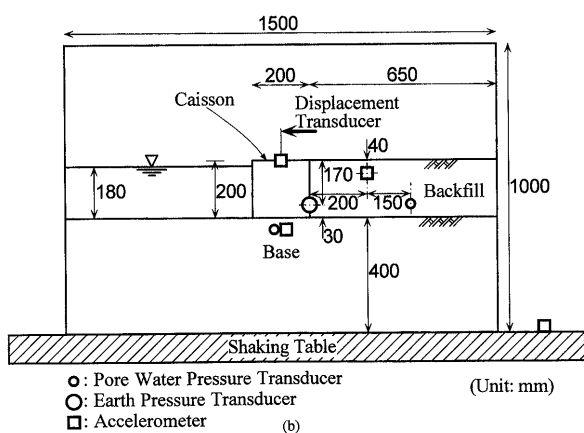
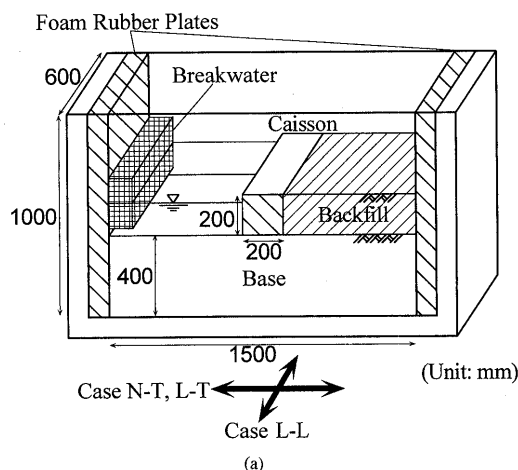


Fig. 2. Schematic figure of shaking table test: (a) model quay wall on shaking table; (b) arrangement of measuring devices

tainer of about 500 kg in mass was fixed on the shaking table in the parallel or perpendicular direction with respect to the direction of shaking. The specifications of the shaking table are shown in Table 1.

Model Preparation

Both the base underlying the caisson and the backfill ground were made with the same siliceous sand whose physical properties are listed in Table 2. Grain size distribution is shown in Fig. 3. Both conventional triaxial compression tests and cyclic undrained triaxial tests were carried out in order to obtain the mechanical properties,

Table 1. Shaking table specifications

Shaking direction	Horizontal one-direction
Control method	Electro-dynamic actuator
Table size	2.5 m × 2.5 m
Table weight	88 kN
Power	Sinusoidal wave 2.5 × 10 ⁶ kg · Gal Random wave 1.0 × 10 ⁶ kg · Gal
Range of frequency	0.1 ~ 100 Hz
Maximum amplitude	100 mm
Maximum velocity	50 cm/sec
Maximum acceleration	2.8 × 10 ³ Gal

Table 2. Physical properties of siliceous sand

Grain density ρ_s	Mean diameter D_{50}	Uniformity coefficient, U_c	Maximum density, ρ_{dmax}	Minimum density, ρ_{dmin}
2.72 g/cm ³	0.18 mm	1.82	1.61 g/cm ³	1.261 g/cm ³

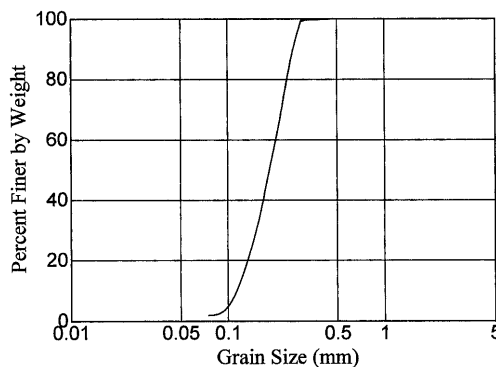


Fig. 3. Grain size distribution curve of sand

which are listed in Table 3. In order to simulate the formation of the foundation and the backfill in the shaking table test, the triaxial specimens were prepared by the water deposition method, where the sand material was deposited in the water filled in the specimen mold. Here, σ_d denotes axial stress amplitude, and σ'_c denotes initial effective confining stress that was kept constant at 49 kPa

Table 3. Mechanical properties of sand

Relative density, D_r (%)	Density of saturated sand, ρ_{sat} (t/m ³)	Internal friction angle, ϕ (deg) from triaxial compression test ($\sigma'_c = 49$ kPa)	Liquefaction strength $\sigma_d/2\sigma'_c$ ($N_c=20, \Delta u/\sigma'_c=0.95$) from cyclic undrained triaxial test ($\sigma'_c=49$ kPa)
30	1.850	33.1	0.096
50	1.892	34.8	0.145
70	1.938	36.2	0.202
90	1.990	38.2	0.238

in all the undrained cyclic loading tests. Results of the cyclic undrained test are shown in Fig. 4 under various criteria on the onset of the liquefaction, among which the criterion based on 95% of excess pore water pressure generation in 20 cycles of loading is indicated in Table 3 as liquefaction strength.

The sand was deposited under the water in order to obtain the sufficient degree of saturation (Kiku, 1993); this method is schematically shown in Fig. 5. When making

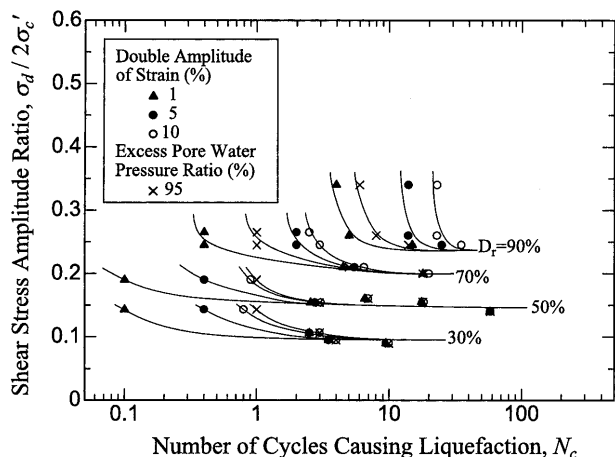


Fig. 4. Liquefaction potential of sand with relative density of 30, 50, 70 and 90%

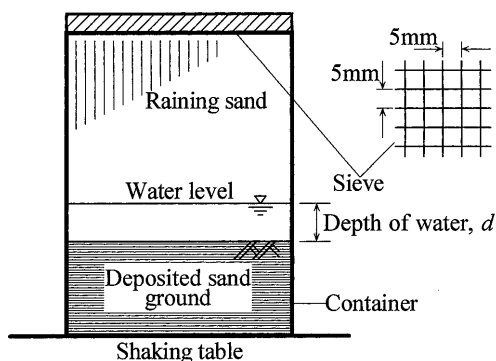


Fig. 5. Water deposition method for preparation of backfill ground

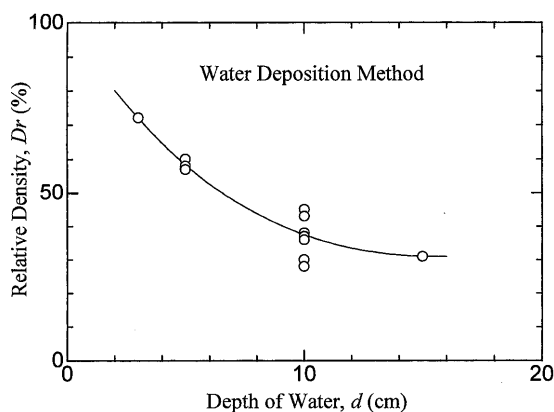


Fig. 6. Relationship between relative density of backfill ground and water depth in water deposition method

the base ground, the base was vibrated intermittently in order to attain a relative density higher than 90%. The density of the backfill was set to be either loose with

Table 4. Backfill conditions in Series B and C tests

Backfill	Comment
Loose sand	$D_r=30-40\%$
Medium sand	$D_r=50-60\%$
Dence sand	$D_r=70-80\%$
Water	Filled with water instead of sand
No backfill	No water at both sides of caisson

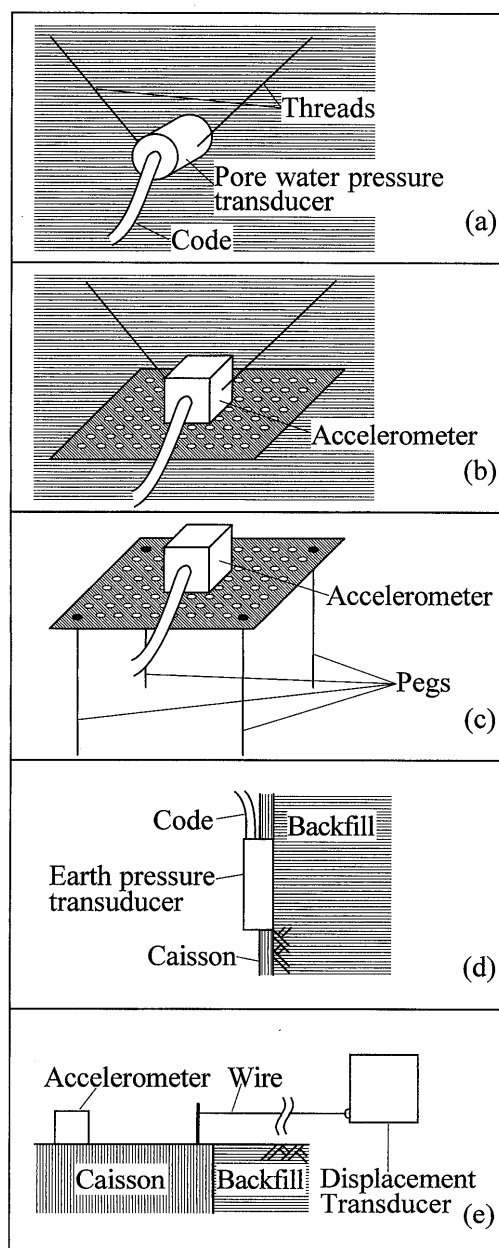


Fig. 7. Installation of measuring devices: (a) pore water pressure transducer under ground; (b) accelerometer under ground; (c) accelerometer on ground surface; (d) total earth pressure transducer on surface of back wall of caisson; (e) wire type displacement transducer for measuring horizontal displacement of caisson

$D_r=30-40\%$, medium with $D_r=50-60\%$, or dense with $D_r=70-80\%$, by changing the depth of the water d in Fig. 5. The relationship between D_r and d is shown in Fig. 6. The model quay walls used in this study, including the one without backfill, are classified into the 5 types shown in Table 4.

Pore water pressure, acceleration, displacement and earth pressure on the caisson were measured with strain gauge type devices whose locations are shown in Fig. 2(b). Pore water pressure transducers were installed in the base and the backfill; the values measured by these transducers are referred to as u_b and u_g , respectively. The devices placed under the ground were suspended by threads as shown in Fig. 7(a), in order to keep their original positions even if liquefaction occurred. The accelerometers were supported in the backfill with thin percolative plate and threads, in order to maintain their original positions and attitudes, as shown in Fig. 7(b, c). An earth pressure transducer was installed on the caisson back wall, as shown in Fig. 7(d), and its value is referred to as p_e . Although pore water pressure was also measured at the back wall, its repeatability and reliability were not sufficient, unlike the total stress, which is therefore the concern of this study. The horizontal displacement of caisson x_c was monitored with a wire type displacement transducer as shown in Fig. 7(e).

Test Program

Three series of model shaking tests were conducted. They are as follows:

- Series A test was planned to focus on the stability of the quay wall caisson against liquefaction in the backfill. Three test cases listed in Table 5 were performed. A sinusoidal acceleration of 220 Gal in amplitude and 2.5 Hz in frequency was used for the base motion.
- Series B test was conducted to obtain the earth pressure from the liquefied ground, especially focusing on the transient earth pressure in the process to liquefaction. Five types of backfill listed in Table 4 were selected to be the parameters. A wide range of magnitude and frequency of the sinusoidal acceleration was applied; the amplitude was 25, 50, 100 or 200 Gal and the frequency was 3, 10, 20 or 40 Hz.
- Series C test was planned in order to grasp the basic vibration characteristics of the quay wall by vibrating the quay wall under high frequency excitation. Two types of models, one with a backfill ground with dense

sand and the other with no backfill, were subjected to a sinusoidal base acceleration of 50 Gal in amplitude and with frequencies between 20 and 80 Hz.

EXPERIMENTAL AND ANALYTICAL INVESTIGATIONS

Effect of Liquefaction on the Stability of Caisson

The behavior in the Series A test is examined in this section. Three test cases listed in Table 5 were named showing the direction of the shaking and occurrence of the liquefaction in the backfill. The first characters 'L' and 'N' indicate whether liquefaction occurred in the backfill or not, respectively. The second characters indicate the direction of the shaking with respect to the longitudinal direction of the caisson: 'T' for transversal direction and 'L' for longitudinal direction.

Time histories of the total earth pressure p_e , inertial acceleration ($-\ddot{x}_b$) and displacement x_c of the caisson are shown in Fig. 8. Figure 9 shows time histories of the ac-

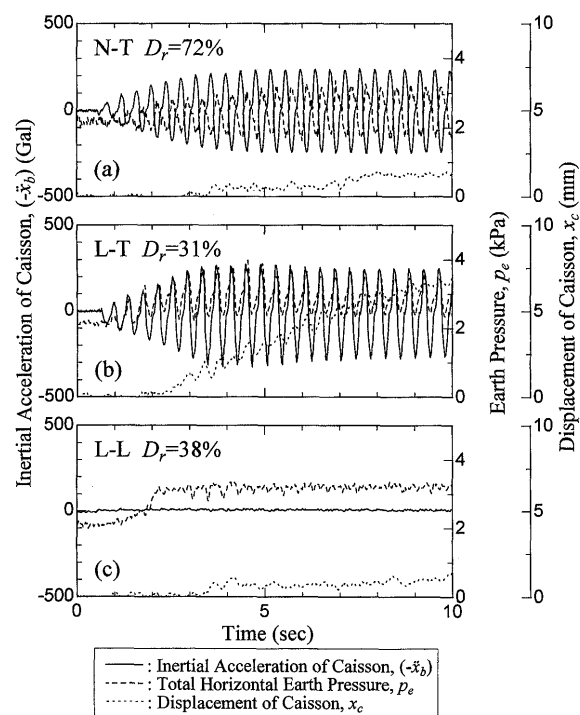


Fig. 8. Time histories of inertial acceleration of caisson ($-\ddot{x}_b$), earth pressure p_e and displacement of caisson x_c : (a) Case N-T; (b) Case L-T; (c) Case L-L

Table 5. Test cases for Series A test

Test case	Relative density, D_r (%)	Liquefaction	Vibration direction	Safety factor against sliding F_s	
				Ordinary	Earthquake ($k_h=0.224$)
N-T	72	No liquefaction	Transverse	2.98	0.65
L-T	31	Liquefaction	Transverse	2.95	0.63
L-L	38	Liquefaction	Longitudinal	2.95	—

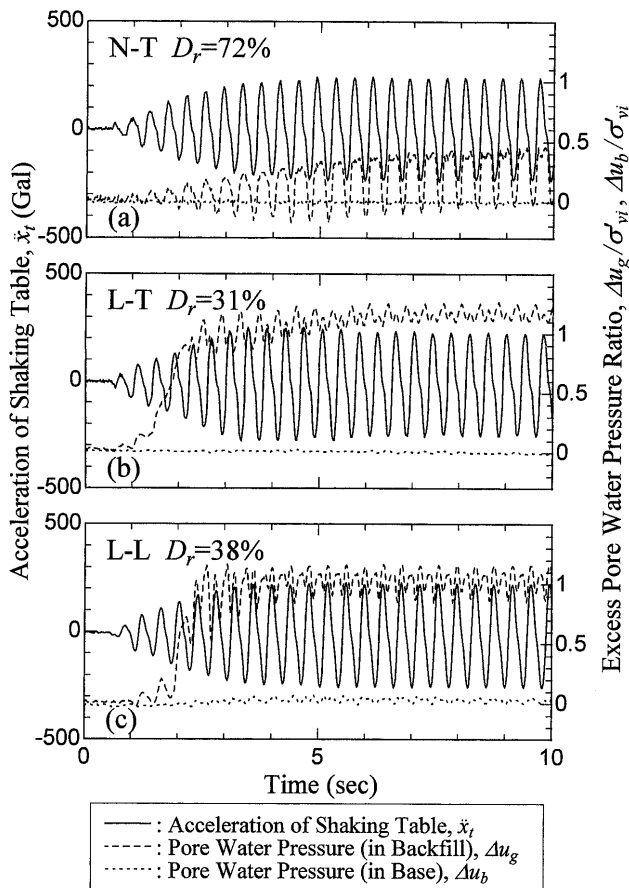


Fig. 9. Time histories of acceleration of shaking table \ddot{x}_t , and pore water pressure at backfill u_g and beneath caisson in base u_b , measured in: (a) Case N-T; (b) Case L-T; (c) Case L-L

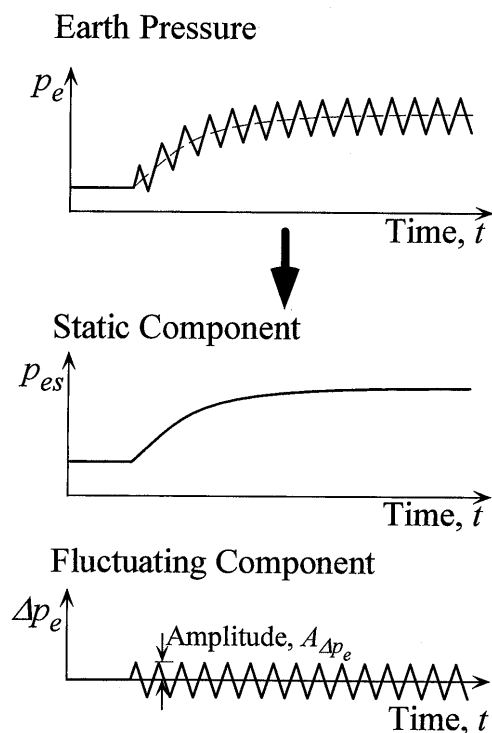


Fig. 10. Definition of static and fluctuating components of earth pressure p_e

celeration at the shaking table \ddot{x}_t , and pore waters u_g and u_b . The measured displacement, accelerations, and inertial forces were designated as positive in the direction toward the sea from the backfill. The definition of the static and fluctuating components of the earth pressure are explained in Fig. 10.

Acceleration \ddot{x}_c was not detected in Case L-L because the direction of the vibration was perpendicular to the direction of measurement. Earth pressure p_e did not fluctuate in this case, although it increased from ordinary to liquefied states monotonically. On the other hand, in Cases N-T and L-T, \ddot{x}_c was obviously detected and the earth pressure increased with fluctuation. Pore water pressure u_g increased in a similar manner in both Cases L-T and L-L, as shown in Fig. 9(b, c). Excess pore water pressure ratio $\Delta u_g / \sigma'_{vi}$, the ratio of the excess pore water pressure Δu_g to the initial effective overburden stress σ'_{vi} , increased up to unity within 3 seconds from the start of the vibration, indicating the occurrence of liquefaction in the backfill. On the other hand, the time history of $\Delta u_g / \sigma'_{vi}$ in Case N-T indicates that liquefaction did not occur in the backfill. Pore water pressure increased with fluctuation, but the maximum value was only a half of the initial effective overburden stress, because liquefaction strength was very large, as shown in Fig. 4 and Table 3.

Time histories of the accelerations \ddot{x}_c , \ddot{x}_b and \ddot{x}_t in Cases N-T and L-T are shown in Fig. 11, where components the same as the input motion (2.50 Hz) were retrieved from the measured time history around 6 seconds after the beginning of shaking, in order to make discussion easy. All

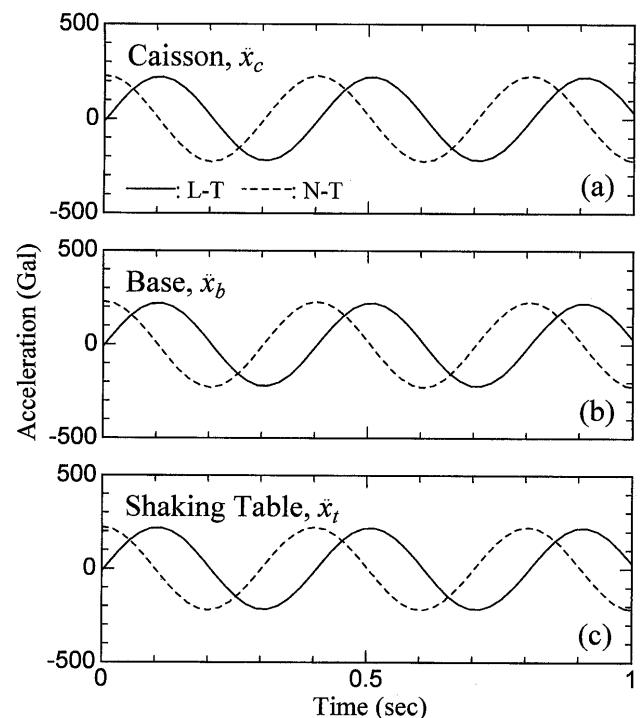


Fig. 11. Time histories of measured inertial accelerations around 6 seconds after beginning of shaking in Case N-T and Case L-T: (a) top of caisson \ddot{x}_c ; (b) base beneath caisson \ddot{x}_b ; (c) shaking table \ddot{x}_t . Note that dashed lines are sifted by 90 deg. phase angle in the horizontal direction

the wave forms in different cases and at different locations are almost the same, and it is noted that the phase difference between Cases N-T and L-T is artificially set by moving the time axis in Case N-T. This suggests that both the foundation ground and caisson were sufficiently rigid and resonance between them did not occur. Even in Case L-T where the caisson slid notably, the accelerations measured on the shaking table, base and top of caisson were the same and the rocking mode vibration was not, therefore, recognized. This is also proved by the fact that the accumulation of excess pore water pressure and the reduction in effective vertical stress was negligibly small in the base ground, as shown in Fig. 9.

Figure 8 indicates that the backfill ground liquefied and the effective stress were perfectly lost in Cases L-T and L-L. The caisson, however, moved significantly only in Case L-T. Even in this case, the movement or slide ceased when input acceleration terminated. This indicates that both the inertial force on the caisson and the onset of liquefaction in the backfill are keys in the stability of the caisson under the conditions concerned with in this study.

The stability of the caisson against sliding is evaluated by the seismic coefficient method (Japan Port and Harbor Association, 1989). The safety factor F_s is calculated to be 2.98 in Case N-T and 2.95 in Cases L-T and L-L under the ordinary loading condition under which both active earth pressure and sea water pressure work. They are 0.65 in Case N-T and 0.63 in Case L-T when seismic intensity of $k_h=220/980=0.224$ is considered, where 220 Gal is the amplitude of the base acceleration. The earth pressure increases more when liquefaction occurs in the backfill ground as shown in Fig. 12; F_s becomes, for example, 1.11 even when inertial force is not considered in Case L-L.

Judging from the result of the stability analysis, the caisson could slide during the earthquake even in case N-T ($F_s=0.65$). The displacement of the caisson was, however, very small at only 3 mm or 2% of the height of the caisson. This indicates that both inertial force and liquefaction of the backfill are necessary to cause instabil-

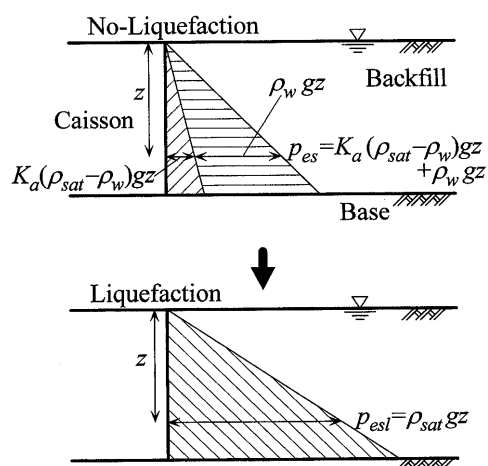


Fig. 12. Rise in static earth pressure p_e due to liquefaction

ity in the caisson. Comparison of the behaviors between Case L-T and Case L-L suggests that the dynamic earth pressure plays an important role in the stability of the caisson. These experimental results agree with the trend of the actual damage to quay walls during the earthquake. For example, displacement of the caisson in Port Island damaged during the 1995 Hyogoken-nambu earthquake is reported to be larger in the direction of the predominant shaking than the minor direction (Inagaki et al., 1996).

The relationships between the inertial acceleration ($-\ddot{x}_b$) and earth pressures p_e are plotted in Fig. 13 during 1 cycle around 6 seconds from the beginning of vibration. In Case L-L, neither ($-\ddot{x}_b$) nor p_e fluctuated; only a rise in p_e caused by the occurrence of liquefaction is seen (see Figs. 8(c) and 12). The same amount of rise in p_{es} is also observed in Case L-T.

Both ($-\ddot{x}_b$) and p_e oscillated in Cases N-T and L-T, but the orientations of the loops are clearly different from each other. This difference is also seen in Fig. 14 in which the predominant components of ($-\ddot{x}_b$) and fluctuating component of the earth pressure Δp_e around 6 seconds after the beginning of shaking are shown. The directions of ($-\ddot{x}_b$) and Δp_e are almost opposite in Case N-T, but almost the same in Case L-T. The reason why instability of the caisson occurred only in Case L-T is explained from this contrast; both inertial force and earth pressure act in the same direction at the same time in Case L-T.

The forces acting on the caisson during the vibration are illustrated in Fig. 15. The four cases shown in the figure have the following characteristics:

- Case A—Figure 15(a) shows the inertial force F_i acting on the caisson; the existence of the sea water and backfill ground is neglected. The outward inertial force F_i reaches peak at state (A).
- Case B—Figure 15(b) shows the inertial force F_i , static components of resultant sea water pressure F_{ws} and resultant backfill earth pressure F_{es} ; fluctuating components of the pressures ΔF_w and

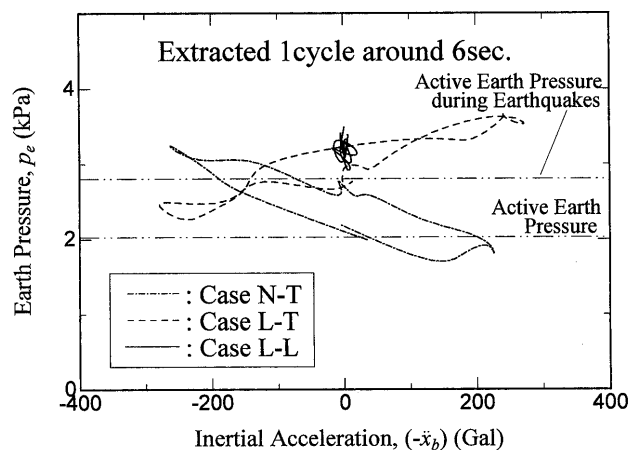


Fig. 13. Cyclic fluctuation of inertial acceleration ($-\ddot{x}_b$) and earth pressure p_e measured around 6 seconds after beginning of shaking in Cases N-T, L-T and L-L

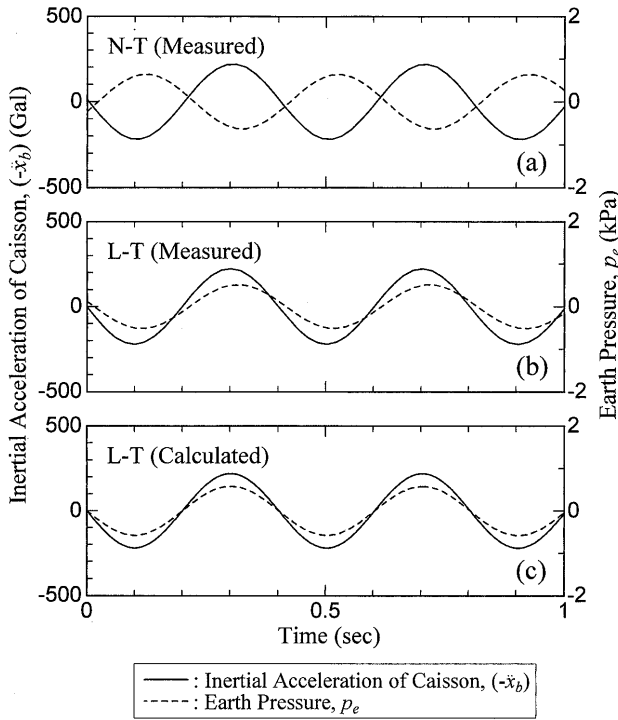


Fig. 14. Dominant components of inertial acceleration ($-\ddot{x}_b$) and earth pressure p_e analyzed from time histories around 6 seconds after beginning of shaking: (a) measured in case N-T; (b) measured in case L-T; (c) calculated for case L-T based on Westergaard's formula

ΔF_e are neglected. Since F_{es} includes static pore water pressure ($=F_{ws}$) and is therefore larger than F_{ws} , the maximum resultant force $F_{r\max}$ increases by the amount of $F_{es}-F_{ws}$ from Case A.

Case C—Figure 15(c) shows the case when liquefaction does not occur, in which both fluctuating components of resultant earth pressure ΔF_e and resultant sea water pressure ΔF_w are considered in addition to the forces in Case B. Based on the test results shown in Figs. 13 and 14(a), ΔF_e works in the opposite direction to F_i . As a result, the maximum resultant force $F_{r\max}$ becomes smaller than that in Case B; therefore the caisson becomes more stable than Case B.

Case D—Figure 15(d) shows the case when liquefaction occurs, in which both ΔF_e and ΔF_w are again considered. The test results shown in Figs. 13 and 14(b) indicate that the static component of the earth pressure p_{es} increases and the directions of ($-\ddot{x}_b$) and Δp_e coincide. The maximum resultant force $F_{r\max}$, therefore, increases from Case B, and the caisson becomes more unstable than Case B, in contrast to Case C.

Earth Pressure from Liquefied Backfill Ground

If perfect liquefaction occurs, soils are considered to

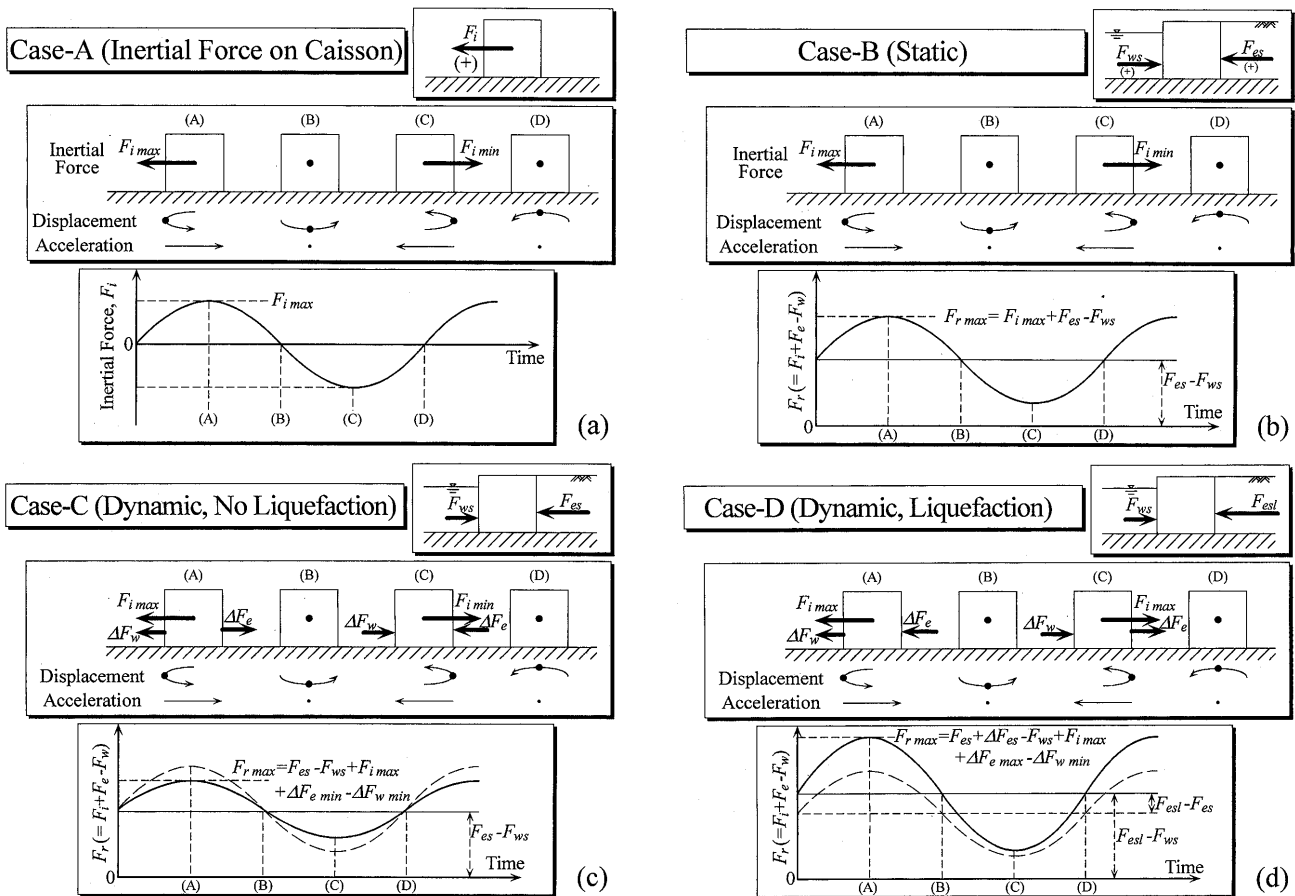


Fig. 15. Illustration of forces to which the model quay wall is subjected: (a) inertial forces F_i ; (b) static components of water F_{ws} and earth pressures F_{es} ; (c) dynamic component ($\Delta F_w, \Delta F_e$) in no-liquefaction case; (d) dynamic component ($\Delta F_w, \Delta F_e$) in liquefaction case

lose their shear stiffness and strength completely and should, therefore, behave like a liquid. To confirm this idea, the fluctuating earth pressure of the liquefied backfill and fluctuating water pressure were investigated through the Series B test.

Test results of this series are shown in Figs. 16 and 17. The measured amplitude of the earth pressure $A_{\Delta p_e}$ is plotted against the amplitude of the inertial acceleration of the caisson $A_{\ddot{x}_b}$ in Fig. 6. A positive correlation is found between $A_{\Delta p_e}$ and $A_{\ddot{x}_b}$ in both cases, i.e., when the backfill ground liquefied and when the back of the caisson was filled with water. Phase angle difference $\Delta\theta_{(\Delta p_e, -\ddot{x}_b)}$ is plotted against $A_{\ddot{x}_b}$ in Fig. 17 in both cases, where $\Delta\theta_{(\Delta p_e, -\ddot{x}_b)}$ is defined as the phase of Δp_e with respect to $(-\ddot{x}_b)$. These figures show a clear contrast between the cases whether liquefaction occurred in the backfill or not; $\Delta\theta_{(\Delta p_e, -\ddot{x}_b)}$ was nearly 0 when liquefaction occurred and is nearly $-\pi$ if liquefaction did not occur. This tendency agrees with the observation in the preceding section in which inertial force and earth pressure were shown to be in the same direction when the backfill ground liquefied and in the opposite direction when it did not.

As examined so far, liquefaction in the backfill affects the behavior of the caisson significantly, and it seems that the backfill ground behaves like a liquid. Therefore, as a first step, we treat the liquefied backfill as a liquid and formulate the behavior analytically.

If backfill ground behaves like a liquid, the dynamic earth pressure may be computed by Westergaard's formula (Westergaard, 1933) originally proposed for the dam.

$$\Delta p_w = \frac{8\alpha\rho h}{\pi^2} \sum \frac{1}{n^2 c_n} \left(\sin \frac{n\pi}{2h} y \right) \exp \left(\frac{2int}{T} \right),$$

$$c_n = \sqrt{1 - \frac{16H^2\rho}{n^2 k T^2}} \quad (1)$$

or a simplified form obtained through a numerical best fit by parabolic equation,

$$A_{\Delta p_w} = \frac{7\alpha\rho}{8} \sqrt{Hy} \quad (2)$$

where $A_{\Delta p_w}$ is the amplitude of fluctuating water pres-

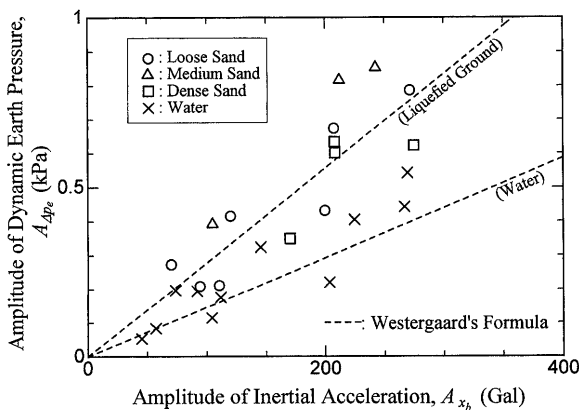


Fig. 16. Amplitude of fluctuating earth pressure $A_{\Delta p_e}$ vs. inertial acceleration amplitude $A_{\ddot{x}_b}$ relationship, compared with calculated values based on Westergaard's formula

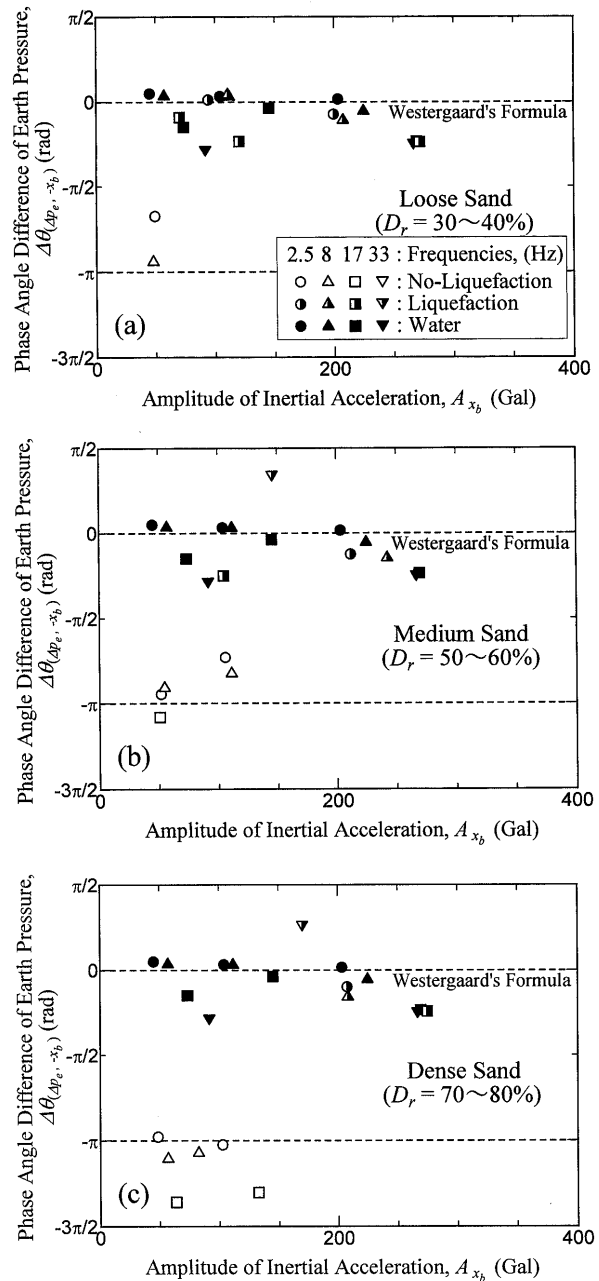


Fig. 17. Phase angle difference $\Delta\theta_{(\Delta p_e, -\ddot{x}_b)}$ between earth pressure and inertial force vs. inertial acceleration amplitude $A_{\ddot{x}_b}$ relationships for: (a) loose sand ($D_r=30\sim40\%$); (b) medium sand ($D_r=50\sim60\%$); (c) dense sand ($D_r=70\sim80\%$)

sure, α and T are amplitude and period of the base sinusoidal acceleration wave, respectively, H is the depth of dam reservoir, and y is the coordinate measured downward from the water surface. Parameters ρ and K are mass density and bulk modulus of the reserved water, respectively.

In the perfectly liquefied condition, it was assumed that the water table rose up to the ground surface, and the overall backfill liquefied. Figure 14(c) shows calculated fluctuating earth pressure from Eq. (1), in which H is the thickness of the backfill of 20 cm, ρ is set to be ρ_{sat} and K to be 0.933×10^5 kPa, which are typical values for loose sand (JSCE, 1994). It should be noted that the

value of K is not important in calculating the earth pressure under ordinary condition; this can be confirmed because K does not appear in Eq. (2).

Measured earth pressures under a wide range of frequency and magnitude of base acceleration are compared with those by Westergaard's formula in Figs. 16 and 17. The Westergaard's solution agrees with the measured earth pressure in both amplitude and phase when liquefaction occurred at the backfill. As pointed out by Westergaard (1933), Δp_e is the same in phase angle with $(-\dot{x}_b)$, therefore fluctuation of the water pressure during the earthquake notably reduces the stability of the caisson. This is why the onset of liquefaction causes severe damage to caisson quay walls; it is therefore an important factor in earthquake resistant design.

Earth Pressure in the Process to Liquefaction

Through the discussion in the previous sections, it becomes clear that, if liquefaction occurs, the backfill ground behaves like a liquid and the behavior is quite different when liquefaction does not occur. The next question to arise is when does the change occur; during the process to liquefaction or just at the onset of liquefaction?

Shown in Fig. 18 are the variations of the earth pressure on the caisson during the process to liquefaction in the backfill, obtained from the Series B test. In these figures static earth pressure p_{es} , amplitude of fluctuating component of earth pressure $A_{\Delta p_e}$ normalized by that of dynamic water pressure from the liquefied backfill calculated by Westergaard's formula (Eq. (1)) A_{pw} , and phase angle difference $\Delta\theta_{(\Delta p_e, -\dot{x}_b)}$ are plotted against the excess pore water pressure ratio $\Delta u_g / \sigma'_{vi}$. It should be noted that all the backfill ground liquefied apart from dense sand backfill, and sinusoidal base acceleration \dot{x}_b is 40 Hz in frequency and 50 Gal in amplitude; this can be recognized because $\Delta u_g / \sigma'_{vi}$ reached unity.

Static earth pressure p_{es} rises monotonically and linearly from initial active pressure to p_{est} . Normalized amplitude $A_{\Delta p_e} / A_{pw}$ first reduces significantly to a fairly small value of about one tenth of initial values, then increases suddenly up to the values calculated from Westergaard's solution according to the excess pore water pressure generation. Under the test condition employed in this study, the minimum values of $A_{\Delta p_e}$ are attained in the region of $\Delta u_g / \sigma'_{vi}$ between 0.8 and 0.95. Phase angle difference $\Delta\theta_{(\Delta p_e, -\dot{x}_b)}$ is almost $-\pi$ although it scatters a little, and leaps to 0 together with the sudden increase of $A_{\Delta p_e}$ as seen in Fig. 18(b, c). This indicates that the ground begins to behave like a liquid when effective mean stress reduces to a certain amount.

A simplified mass-spring-dashpot model is devised in order to explain the transient behavior of the caisson-backfill ground system in the process to liquefaction. The caisson and backfill ground are modeled into lumped masses whose mass are m_c and m_g . They are connected with a spring with a spring constant of k_i and a dashpot with a viscous coefficient of c_i . The base input motion $x_b(=X_b \exp(i\omega_b t))$ is propagated into the caisson and

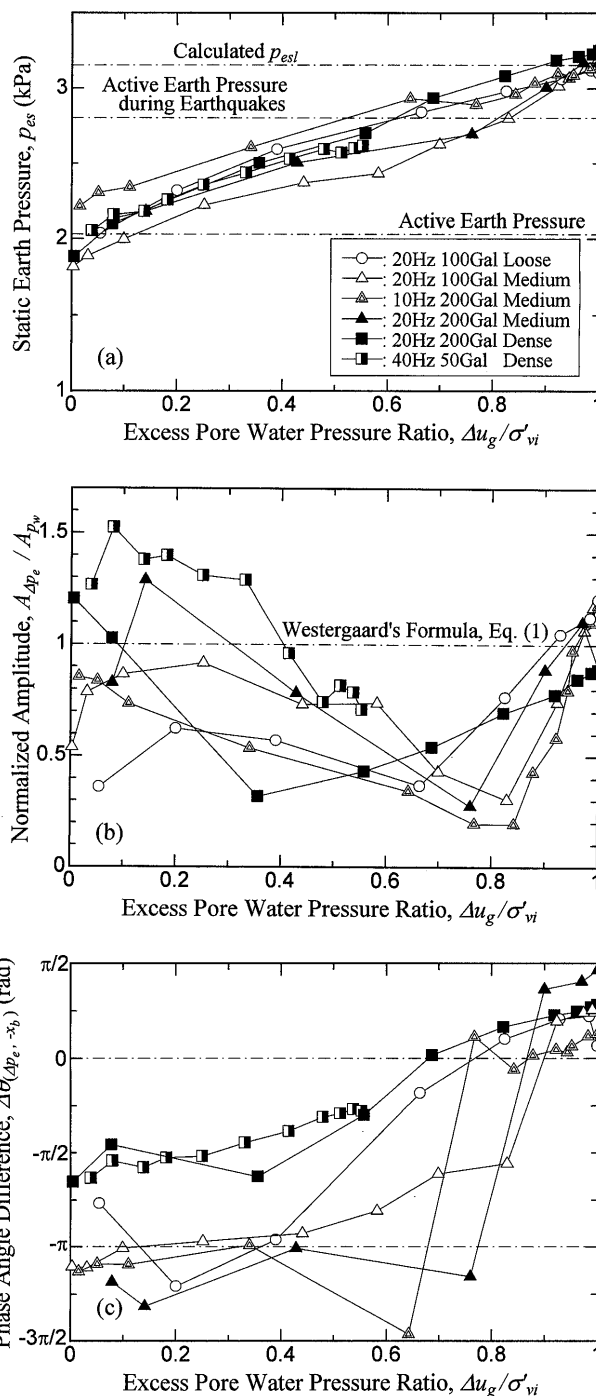


Fig. 18. Variation of measured earth pressure during process of liquefaction: (a) static component p_{es} ; (b) amplitude $A_{\Delta p_e} / (A_{F1} / H)$; (c) phase angle difference $\Delta\theta_{(\Delta p_e, -\dot{x}_b)}$

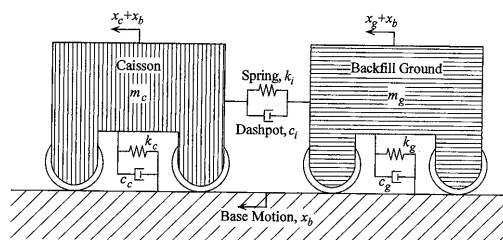


Fig. 19. Simplified mass-spring-dashpot model for simulation of transient dynamic earth pressure

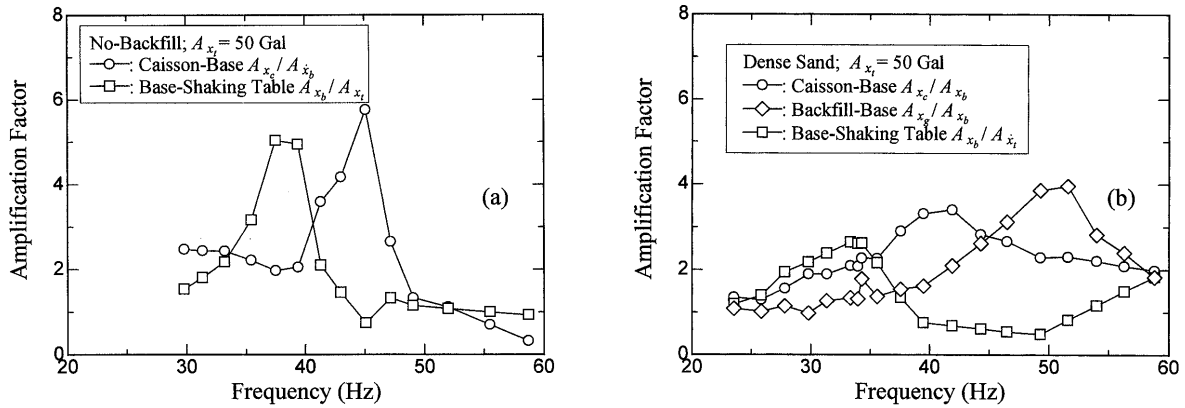


Fig. 20. Basic vibration properties of base, caisson and backfill: relationship of amplification factor with frequency of base acceleration

the backfill through the springs (k_c , k_g) and dashpots (c_c , c_g) as shown in Fig. 19. The natural angular frequencies ω , critical damping ratio h and complex spring coefficients K are defined as follows:

$$\omega_c = \sqrt{k_c/m_c}, \quad h_c = c_c/\sqrt{4m_c k_c}, \quad K_c = k_c + i\omega_b c_c \quad (3)$$

$$\omega_g = \sqrt{k_g/m_g}, \quad h_g = c_g/\sqrt{4m_g k_g}, \quad K_g = k_g + i\omega_b c_g \quad (4)$$

$$\omega_i = \sqrt{k_i/m_c}, \quad h_i = c_i/\sqrt{4m_c k_i}, \quad K_i = k_i + i\omega_b c_i \quad (5)$$

where suffixes 'b', 'c', 'g' and 'i' correspond to the parameters for base, caisson, backfill ground and the interface between caisson and backfill ground, respectively, and ω_b is the angular frequency of the base motion. A simultaneous momentum equation for the model is given by

$$\begin{bmatrix} -\omega_b^2 m_c + K_c + K_i & -K_i \\ -K_i & -\omega_b^2 m_g + K_g + K_i \end{bmatrix} \begin{Bmatrix} X_c \\ X_g \end{Bmatrix} = \begin{Bmatrix} \omega_b^2 m_c X_b \\ \omega_b^2 m_g X_b \end{Bmatrix} \quad (6)$$

where $x_c (= X_c \exp(i\omega_b t))$ and $x_g (= X_g \exp(i\omega_b t))$ are relative displacements of the caisson and backfill ground, respectively. The inertial force F_i to which the caisson is subjected and the force generated at the interface ΔF_e , which corresponds to the earth pressure, are calculated by

$$\begin{aligned} F_i &= m_c \omega_b^2 X_c \exp(i\omega_b t), \\ \Delta F_e &= -K_i (X_c - X_g) \exp(i\omega_b t) \end{aligned} \quad (7)$$

In order to solve Eq. (6), vibration characteristics of the caisson and backfill ground are required. The Series C test was planned to obtain them. The amplification factors at the base, caisson and backfill were computed from the Series C test results, which are shown in Fig. 20. Natural frequencies at base and caisson were about 37 and 45 Hz, respectively when there was no backfill (Fig. 20(a)). They were slightly reduced to about 34 and 43 Hz when there was a backfill with dense sand, as shown in Fig. 20(b). The backfill made of dense sand had a natural frequency of about 52 Hz, as shown in Fig. 20(b). It is noted that the natural frequency of the caisson was smaller than that of the backfill ground. Probably, rock-

Table 6. Mechanical parameters used for simplified mass-spring-dashpot model

ω_g/ω_c :	0.0-3.0
m_g/m_c :	4.0
ω_i/ω_c :	0.25-2.0
ω_b/ω_c :	0.22(=10/45)
$h(=h_c=h_g=h_i)$:	0.2

ing of the caisson is more predominant than shear deformation.

The values of the mechanical parameters used in the simulation are listed in Table 6. The frequency of the sinusoidal base motion was 10 Hz. The same value of h of 0.2 was used for all the spring-dashpot systems. Spring constant at the interface k_i were parametrically varied in the simulation. The results of the parametric calculation are shown in Fig. 21; the amplitude of the earth pressure normalized by the inertial force $A_{\Delta F_e}/A_{F_i}$ and phase angle difference $\Delta\theta_{(\Delta F_e, F_i)}$ are plotted against the ratio of the natural angular frequency of backfill ground ω_g to that of caisson ω_c . The reduction of the natural frequency ratio ω_g/ω_c corresponds to the reduction of the stiffness of backfill ground due to the generation of pore water pressure in the process to liquefaction. As shown in these figures the amplitude of the earth pressure first descends and vanishes when the natural frequencies of the caisson and backfill coincide, i.e., $\omega_g/\omega_c=1$. Then it starts to ascend. The phase angle difference leaps from around $-\pi$ to around 0 at $\omega_g/\omega_c=1$ or the amplitude $A_{\Delta F_e}$ equals 0. Comparison between Figs. 18(b, c) and 21 shows that the transient feature of the earth pressure in the process to liquefaction is simulated qualitatively by the analysis.

CONCLUSION

Series of model shaking table tests were conducted in order to investigate the damage mechanism of gravity type quay walls during earthquakes, especially focusing on the occurrence of liquefaction in the backfill ground.

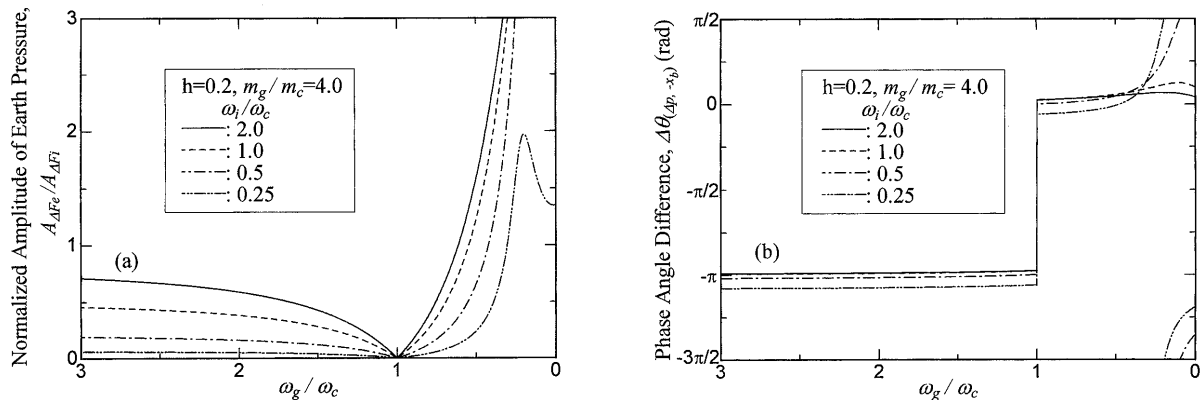


Fig. 21. Simulated resultant fluctuating earth pressure during process to liquefaction: (a) amplitude $A_{\Delta P_e}$; (b) phase angle difference $\Delta \theta_{(\Delta P_e, F_i)}$

The following conclusions are obtained from observation of the test results and simplified analysis.

- The sliding of the caisson is largely enhanced when liquefaction occurs in the backfill ground. The caisson becomes unstable the most easily when vibrated in the transversal direction, because three components, increase in the static component of the earth pressure induced by liquefaction, fluctuation of the earth pressure from the liquefied backfill and inertial force, all cooperate together to slide the caisson.
- If liquefaction does not occur in the backfill, the fluctuating component of the earth pressure works in the opposite direction to that of the inertial force, therefore sliding is suppressed.
- Dynamic earth pressure with fluctuation from the liquefied backfill can be evaluated by Westergaard's formula. Both the measured and calculated fluctuating earth pressures are in good accordance in amplitude and phase angle.
- When a caisson-backfill ground system is subjected to earthquake load, the amplitude of the earth pressure at the caisson first decreases as excess pore water pressure generates. It reaches a minimum value when the natural period of the backfill ground becomes equal to that of the caisson. After that, according to the softening of the backfill ground, the amplitude increases rapidly and the phase difference leaps to 0, both of which work to make sliding easy.
- The vibration characteristics of the caisson-backfill ground system is confirmed through both experimental and analytical investigations. The stability criterion of gravity type caisson should be discussed by the onset of liquefaction in the backfill and the liquefaction associated sudden phase change between the earth pressure and inertial force, as well as by the inertial force. According to the observation in the experiment, the threshold state corresponds to excess pore water pressure generation of about 80 to 95% of the initial overburden stress. As described in the previous item, however, the threshold state should be described by the coincidence of the predominant period between the caisson and the backfill ground, but not by the amount of excess pore water pressure generation. In order to

develop these criteria, more detailed investigations and measurement of actual caissons will be required because the vibration characteristics of caissons are complicated, including shear and rocking behavior.

- A simple mass-spring-dashpot system proposed here is shown to have the possibility to evaluate the dynamic earth pressure during the process to liquefaction in the backfill ground.
- The results of experimental and analytical investigations obtained in this study indicate that the remedial treatment of backfill ground against liquefaction significantly improves the stability of a quay wall during earthquake. This suggests the possibility of the rational and economical earthquake proof design of gravity type quay walls based on the vibration characteristics of the caisson and the backfill ground.
- Both the inertial force acting on the caisson and earth pressure from the backfill ground are considered simultaneously in the earthquake resistant design of the caissons at present. The findings in this paper, however, suggest that a more rational and economical design is possible in gravity type quay walls with sufficient remedial counter measure against liquefaction if the vibration characteristics of the caisson and the backfill ground are considered.

ACKNOWLEDGEMENT

The authors are grateful to Messrs. Takahiko Sasajima and Sadamitsu Akeda of Hokkaido Development Bureau for their support. They are also grateful to Prof. Susumu Yasuda of Tokyo Denki University for his technical advice on the shaking table test, and to Messrs. Nobukatsu Oka and Kazuma Harada for their help conducting the experiment and processing data. They would like to express their sincere thanks to Prof. Shosuke Toki of Hokkaido Institute of Technology for his continued encouragement.

NOTATION

- α : normalized amplitude of base acceleration with respect to the gravity acceleration g in Westergaard's formula

gaard's formula
 $\Delta\theta$: general expression of phase angle difference
 $\Delta\theta_{(\Delta p, -\dot{x}_b)}, \Delta\theta_{(\Delta p, -F)}$: phase angle difference of fluctuating earth pressure with respect to inertial force and, inertial force; $\Delta\theta_{(\Delta p, -\dot{x}_b)} = \Delta\theta_{(\Delta p, -F)}$
 ρ : density of reservoir water in Westergaard's formula [ML^{-3}]
 ρ_{sat} : density of saturated sand materials of base and background [ML^{-3}]
 ρ_w : density of sea water [ML^{-3}]
 σ'_{vi} : initial effective vertical stress [$ML^{-1}T^{-2}$]
 ω_b : angular frequency of base [MT^{-1}]
 $\omega_c, \omega_g, \omega_i$: natural angular frequencies for caisson, background and interface [MT^{-1}]
 A : general expression of amplitude
 $A_{Fi}, A_{\Delta Fi}$: amplitudes of inertial force and resultant fluctuating earth pressure [MLT^{-2}, MLT^{-2}]
 $A\Delta p_e, A\dot{x}_b$: amplitudes of fluctuating earth pressure and base accelerations [$ML^{-1}T^{-2}, LT^{-2}$]
 c_c, c_g, c_i : dashpot coefficients for caisson, background and interface [MT^{-1}]
 d : depth of water in water deposition method [L]
 D_r : relative density
 F_i : inertial force on caisson [MLT^{-2}]
 F_e, F_w : resultant earth pressure and sea water pressure on caisson [MLT^{-2}]
 F_{es}, F_{ws} : static components of resultant earth pressure and sea water pressure on caisson [MLT^{-2}]
 F_{esi} : static components of resultant earth pressure from liquefied backfill [MLT^{-2}]
 $\Delta F_e, \Delta F_w$: fluctuating components of resultant earth pressure and sea water pressure on caisson [MLT^{-2}]
 F_r : resultant force on caisson [MLT^{-2}]
 F_{rmax} : maximum resultant force on caisson [MLT^{-2}]
 F_s : safety factor against slide
 g : gravity acceleration [LT^{-2}]
 h : general expression of critical damping ratio
 h_c, h_g, h_i : critical damping ratio for caisson, background and interface
 H : depth of dam reservoir in Westergaard's formula or height of caisson [L]
 K : bulk modulus of reservoir water in Westergaard's formula [$ML^{-1}T^{-2}$]
 k_c, k_g, k_i : spring coefficients for caisson, background and interface [MT^{-2}]
 K_c, K_g, K_i : complex expressions of stiffness for caisson, background and interface [MT^{-2}]
 k_h : horizontal seismic coefficient in seismic coefficient method
 m_c, m_g : mass for caisson and background [M]
 p_e : total earth pressure [$ML^{-1}T^{-2}$]
 $p_{es}, \Delta p_e$: static and fluctuating components of earth pressure [$ML^{-1}T^{-2}$]
 p_{esi} : hydrostatic components of earth pressure in liquefaction case [$ML^{-1}T^{-2}$]
 p_w : sea water pressure on caisson [$ML^{-1}T^{-2}$]
 $p_{ws}, \Delta p_w$: static and fluctuating components of sea water pressure [$ML^{-1}T^{-2}$]
 T : time [T]
 T : period of base acceleration in Westergaard's formula [T]
 u_b, u_g : pore water pressures in base and backfill [$ML^{-1}T^{-2}$]
 $\Delta u_b, \Delta u_g$: excess pore water pressures in base and backfill [$ML^{-1}T^{-2}$]

$\Delta u_g / \sigma'_{vi}$: excess pore water pressure ratio to initial effective vertical stress in backfill ground
 x, \dot{x}, \ddot{x} : general expression of displacement, velocity and acceleration [L, LT^{-1}, LT^{-2}]
 x_b, x_c, x_g : displacement of base, and relative displacements of caisson and background [L]
 $(-\ddot{x}_b)$: inertial acceleration of caisson [L, LT^{-1}, LT^{-2}]
 \ddot{x}_i : acceleration of shaking table [L, LT^{-1}, LT^{-2}]
 X_b, X_c, X_g, X_i : complex expressions of displacement of base, and relative displacements of caisson and background [L]
 y : coordinate measured downward from the reservoir surface Westergaard's formula [L]

REFERENCES

- Hokkaido Development Bureau (1996): "Report on the improvement of the seismic resistance of port facilities," Cold Region Port and Harbor Research Center (in Japanese).
- Inagaki, H., Iai, S., Sugano, T., Yamazaki, H. and Inatomi, T. (1996): "Performance of caisson type quay walls at Kobe Port," Special Issue of Soils and Foundations, pp. 119-136.
- Iwatate, T., Kokusho, T. and Tohma, J. (1982): "Large scaled model vibration tests of embedded shaft considering the effect of soil liquefaction," Central Research Institute of Electric Power Industry, Report No. 381024 (in Japanese).
- Iwatate, T., Tohma, J., Kokusho, T., Kurihara, C. and Ohtomo, K. (1984): "Experimental study of dynamic earth pressure acted on underground structure," Central Research Institute of Electric Power Industry, Report No. 384010 (in Japanese).
- Japan Port and Harbor Association (1989): "Manual for technical standard of port and harbor facilities," (in Japanese).
- JGS (1994): "Report of the damages during 1993 Kushiro-oki and Notohanto-oki earthquakes," pp. 175-182 (in Japanese).
- JSCE (1994): "Coastal wave, -State of the art of the analytical methods of interactions among waves, structures and grounds-, " pp. 481-483 (in Japanese).
- Kamon, M., Wako, T., Isemura, K., Sawa, K., Mimura, M., Tateyama, K. and Kobayashi, S. (1996): "Geotechnical disasters on the waterfront," Special Issue of Soils and Foundations, pp. 137-147.
- Kazama, M. and Inatomi, T. (1990): "Model vibration test for the seismic earth pressure acting on the rigid caisson foundation," Proc. of J. of JSCE, No. 415/I-13, pp. 419-428 (in Japanese).
- Kiku, H. (1993): "A study on the permanent displacement of liquefied ground," Thesis for the Partial Fulfillment for the Degree of Doctor of Engineering, Kitakyushu Institute of Technology (in Japanese).
- Matsuo, H. (1941): "Experimental study on the distribution of seismic earth pressure on retaining wall," Journal of ASCE, Vol. 27, No. 2, pp. 87-106 (in Japanese).
- Ichihara, M. and Matsuzawa, H. (1972): "Earth pressure during earthquake," Soils and Foundations, Vol. 13, No. 4, pp. 75-86.
- Mononobe, N. (1929): "Earthquake-proof construction of masonry dams," Proc. of the World Engrg. Conf., Vol. 9, p. 275.
- Okabe (1924): "General theory on earth pressure and seismic stability of retaining wall and dam," J. of JSCE, Vol. 10, No. 6, pp. 1277-1323.
- Westergaard, H. M. (1933): "Water pressures on dams during earthquakes," Trans. ASCE, Vol. 98, pp. 418-432.
- Yoshimi, Y. (1985): "Liquefaction of sand grounds", Tsuchi-to-kiso, Japanese Geotechnical Society, Vol. 33, No. 8, pp. 3-8 (in Japanese).